

Auto-, para- and endocrine signalling in modelling & simulation of antibody therapeutics

Kevin Devine¹, Paul Greaney², Lauren Hyndman³, Ahmed Ismaeel⁴,
Louise Mason³, John McGowan⁶, Luca Possenti⁷, Sheila Scialanga⁵

Academic Mentor: Dr Sean McGinty³

Industry Mentor: Dr Armin Sepp⁸

¹MACSI, Department of Mathematics and Statistics, University of Limerick

²School of Mathematics, Statistics and Applied Mathematics,
National University of Ireland, Galway

³Department of Biomedical Engineering, University of Glasgow

⁴Department of Mathematics and Statistics, University of Glasgow

⁵Department of Civil Engineering, University of Glasgow

⁶Department of Mathematics and Statistics, University of Strathclyde

⁷Department of Chemistry, Materials and Chemical Engineering “Giulio Natta”,
Politecnico di Milano

⁸ Drug Metabolism and Pharmacokinetics, GlaxoSmithKline, Stevenage

October 5, 2016

1 Introduction

The use of antibodies in drug design has been a rapidly growing area of research for the past 40 years, with hundreds of drugs now in clinical development for cancer and cardiovascular therapies [1]. The success of this research has led to the production of 8 out of the top 20 biotechnology drugs on the market [2].

An antibody is a large y-shaped protein consisting of two main components, the constant region (*Fc*), and the antigen/receptor binding region (*Fab*), as shown in Figure 1b. The *Fc* binds to the surface of the cell and has similar properties amongst different antibodies [3]. The *Fab* is a variable region with specific molecular functional groups which can interact and bind to a given ligand [4]. The ability of these molecules to bind to highly specific ligands forms the basis for adaptive immune response, leading, for example, to

the neutralisation of harmful pathogens or viruses surrounding the cell such as bacteria [5].

Monoclonal antibodies (*mAbs*) target one specific binding site on an antigen (*Ag*), called an epitope. This mechanism works in a fashion similar to a lock and key mechanism in which there is only one specific antigen that can fit into the binding site of any given antibody. This specificity can be advantageous in drug design as increasing the selectivity to the target of interest can improve therapeutics and help minimise harmful side effects of drugs. In contrast, a polyclonal antibody contains many different antibodies potentially interacting with different epitopes of a given antigen to produce varying cellular outcomes. For the purposes of this study, only monoclonal antibodies will be considered.

Ligand and receptor interactions, such as the *mAb* and *Ag* example can be expressed more generally using the reversible process



where k_f and k_r are rate constants for the forward and reverse reactions, respectively. We define the associated *equilibrium constant*

$$K_D = \frac{k_r}{k_f} = \frac{[mAb][Ag]}{[mAb \cdot Ag]},$$

where the square brackets indicate the concentrations of the respective species. Henceforth we drop the square brackets for convenience.

Three different modes of cell signalling are possible based on the source of the ligand and its corresponding target receptor. In autocrine signalling, ligands bind to receptors on the same cell from which they were secreted, thus establishing an autocrine loop. In contrast, paracrine signalling involves ligands binding to receptors on adjacent cells. Endocrine signalling is more complex with ligands being absorbed into the blood stream by the endocrine gland. These ligands can then travel to other parts of the body to bind to receptors on distant cells. The binding of ligands to receptors, forming receptor-ligand complexes, can be represented by the reversible reaction



with equilibrium constant $K_D = \frac{k_r}{k_f} = \frac{[L][R]}{[L \cdot R]}$. This binding process competes with ligand diffusion and decay.

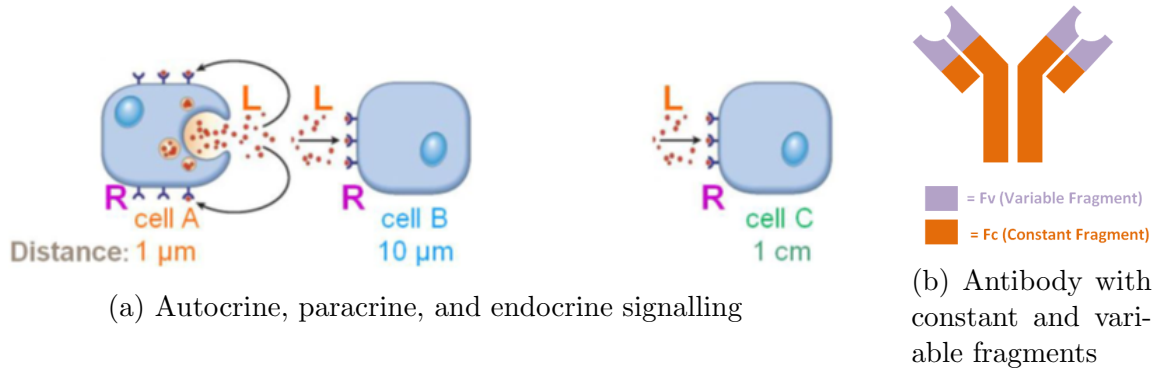


Figure 1: Schematics showing (a) types of signalling and (b) antibody structure

2 Aims

This project aimed to develop mathematical models of ligand-receptor interactions following ligand secretion by cells. Building on this, it is envisaged that the models developed could be expanded to include antibody-mediated interference, and thus used to compare the situations where the *mAb* binds either to the ligand or receptor.

With regard to applying the results to industrial applications, useful calculations which might be addressed using the model include calculation of the ligand secretion rate required to achieve, for example, 90% receptor occupancy on the cell surface in the absence of *mAbs*, and calculation of the global *mAb* concentration and affinities required to reduce receptor occupancy from 90% to 5%.

3 Methodology

3.1 Modelling the chemical reaction

We begin by considering the ordinary differential equation

$$\frac{dC(t)}{dt} = k_f(R_T - C(t))L_0 - k_rC(t), \quad (3)$$

obtained from the reaction (2), where $C = L \cdot R$ represents the concentration of ligand-receptor complexes, R_T is the initial number of receptors on the cell surface, and L_0 is the number of ligands available for binding, which we initially assume to be fixed for convenience. Thus the expression $R_T - C(t)$ represents the number of receptors available for binding at time t . Assuming an initial concentration $C(t = 0) = C_0$, we solve this

equation using the appropriate integrating factor to find

$$C(t) = \frac{k_f R_T L_0}{k_r + k_f L_0} + e^{-(k_r + k_f L_0)t} \left(C_0 - \frac{k_f R_T L_0}{k_r + k_f L_0} \right). \quad (4)$$

The steady state concentration is given by

$$\lim_{t \rightarrow \infty} C(t) = \frac{R_T L_0}{L_0 + K_D},$$

and the time t^* at which a particular value of the saturation concentration C^* is reached is given by

$$t^* = \frac{-1}{k_r + k_f L_0} \ln \left(\frac{C^* - \frac{k_f R_T L_0}{k_r + k_f L_0}}{C_0 - \frac{k_f R_T L_0}{k_r + k_f L_0}} \right). \quad (5)$$

3.2 Modelling ligand diffusion and decay

Assuming an idealised spherical geometry for the cell, we assume that the behaviour of the system is identical in all directions, and so we may simplify the domain to be of one spatial dimension x . We then define $L(x, t)$ to be the concentration of ligands at position x at time $t > 0$, so that the evolution of ligand concentration is governed by the partial differential equation (PDE)

$$\frac{\partial L(x, t)}{\partial t} = D_L \frac{\partial^2 L(x, t)}{\partial x^2} - KL(x, t), \quad 0 < x < \infty, \quad (6)$$

where the first term on the right-hand side accounts for diffusion of ligands with constant diffusivity D_L , and the second for ligand decay at a constant rate K . We suppose that there is a constant number of ligands being emitted from the surface of the cell at a flux rate of J_L , and that all of the ligands eventually decay as they move away from the cell, giving the boundary conditions

$$-D_L \frac{\partial L(x=0, t)}{\partial x} = J_L, \quad t > 0, \quad (7)$$

$$\lim_{x \rightarrow \infty} L(x, t) = 0, \quad t > 0. \quad (8)$$

We further suppose that there are no ligands present in the system initially, so that the appropriate initial condition is

$$L(x, t=0) = 0, \quad 0 < x < \infty. \quad (9)$$

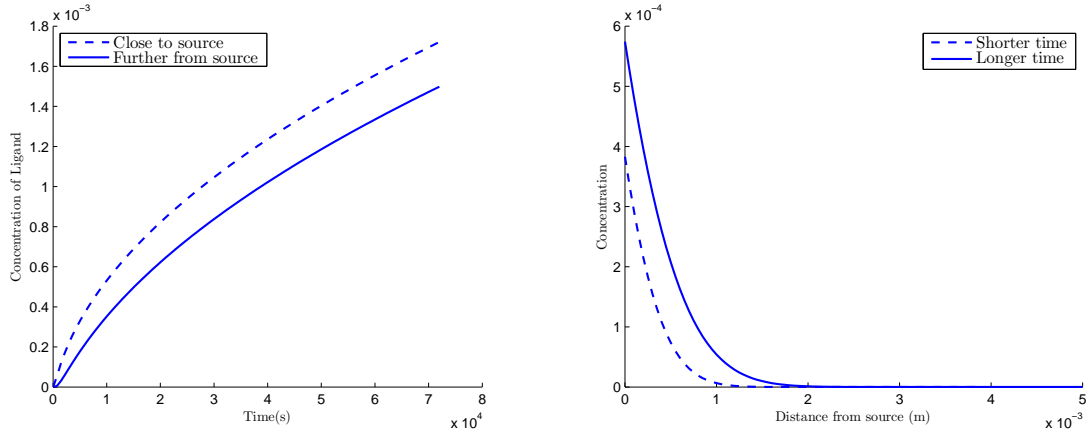


Figure 2: Evolution of ligand concentration $L(x, t)$ for fixed position values (left) and fixed time values (right), in the case where $K = 0$, i.e. no decay is present

The system of equations (6)-(9) may then be solved using a Laplace transform to obtain

$$L(x, t) = \frac{J_L}{2} \sqrt{\frac{D_L}{K}} \left[e^{2\sqrt{Kx^2/D}} \operatorname{erf} \left(\frac{2\sqrt{Kt} + \sqrt{x^2/D}}{2\sqrt{t}} \right) - e^{2\sqrt{Kx^2/D}} + 1 + \operatorname{erf} \left(\frac{2\sqrt{Kt} - \sqrt{x^2/D}}{2\sqrt{t}} \right) \right] e^{-\sqrt{Kx^2/D_L}}, \quad (10)$$

where $\operatorname{erf}(z)$ is the error function.

3.3 Combining reaction with diffusion and decay

We now combine the calculations outlined in the previous two sections to assemble a model describing both the reaction of ligands and receptors, and ligand diffusion and decay. Since ligand-receptor binding only occurs in the presence of receptors, which are located on the cell surface, we restrict the binding process to a domain close to the cell surface at $x = 0$. The binding domain is defined to be of length Δx , and for convenience we assume that the domain over which diffusion and decay occurs is of finite length d , with $\Delta x \ll d$.

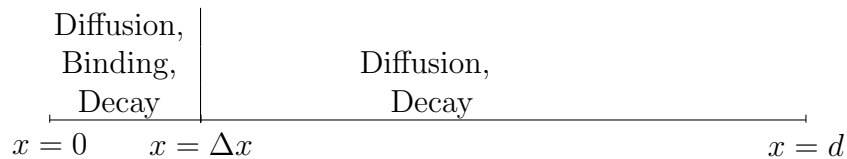


Figure 3: Schematic of domains for diffusion, binding, and decay

We define $L_1(x, t)$ to be the concentration of ligands in $0 < x < \Delta x$, $C(x, t)$ to be the concentration of receptor-ligand complexes in $0 < x < \Delta x$, and $L_2(x, t)$ to be the concentration of ligands in $\Delta x < x < d$. The diffusion and decay of ligands and the binding of ligands with receptors is then described by the system

$$\frac{\partial L_1(x, t)}{\partial t} = D_L \frac{\partial^2 L_1(x, t)}{\partial x^2} - K L_1(x, t) - k_f (R_0 - C(x, t)) L_1(x, t) + k_r C(x, t), \quad 0 < x < \Delta x, \quad (11)$$

$$\frac{\partial C(x, t)}{\partial t} = k_f (R_0 - C(x, t)) L_1(x, t) - k_r C(x, t), \quad 0 < x < \Delta x, \quad (12)$$

where D_L is the constant diffusivity of the ligands, and we have assumed a fixed initial concentration of free receptors R_0 , so that $R = R_0 - C(x, t)$ is the current receptor concentration. The equation describing diffusion and decay outside of the binding region is

$$\frac{\partial L_2(x, t)}{\partial t} = D_L \frac{\partial^2 L_2(x, t)}{\partial x^2} - K L_2(x, t), \quad \Delta x < x < d. \quad (13)$$

The appropriate boundary and initial conditions on L_1, L_2 and C are

$$L_1(x = \Delta x, t) = L_2(x = \Delta x, t), \quad t > 0, \quad (14)$$

$$\frac{\partial L_1(x = \Delta x, t)}{\partial x} = \frac{\partial L_2(x = \Delta x, t)}{\partial x}, \quad t > 0, \quad (15)$$

$$\frac{\partial L_1(x = 0, t)}{\partial x} = -J_L, \quad L_2(x = d, t) = 0, \quad t > 0, \quad (16)$$

$$L_1(x, t = 0) = 0, \quad 0 < x < \Delta x, \quad (17)$$

$$L_2(x, t = 0) = 0, \quad \Delta x < x < d, \quad (18)$$

$$C(x, t = 0) = 0, \quad 0 < x < \Delta x. \quad (19)$$

3.4 Non-dimensionalisation

We now proceed by using dimensional analysis to reduce the number of parameters appearing in the model presented above. We nondimensionalise the lengthscale with the domain length d , the timescale with $\frac{d^2}{D_L}$, and the concentrations with the equilibrium constant K_D , so that the nondimensional variables and concentrations are given by

$$x' = \frac{x}{d}, \quad t' = \frac{D_L}{d^2} t, \quad L'_1 = \frac{L_1}{K_D}, \quad L'_2 = \frac{L_2}{K_D}, \quad C' = \frac{C}{K_D}.$$

Substituting these into equations (11)-(13) and dropping the primes for convenience yields the nondimensionalised system of equations

$$\frac{\partial L_1(x, t)}{\partial t} = \frac{\partial^2 L_1(x, t)}{\partial x^2} - \beta L_1(x, t) - \alpha [(\gamma - C(x, t))L_1(x, t) - C(x, t)], \quad 0 < x < \varepsilon, \quad (20)$$

$$\frac{\partial C(x, t)}{\partial t} = \alpha [(\gamma - C(x, t))L_1(x, t) - C(x, t)], \quad 0 < x < \varepsilon, \quad (21)$$

$$\frac{\partial L_2(x, t)}{\partial t} = \frac{\partial L_2(x, t)}{\partial x^2} - \beta L_2(x, t), \quad \varepsilon < x < 1, \quad (22)$$

with nondimensional parameters

$$\alpha = \frac{k_r d^2}{D_L}, \quad \beta = \frac{K d^2}{D_L}, \quad \gamma = \frac{R_0}{K_D}, \quad \varepsilon = \frac{\Delta x}{d}, \quad Q = -\frac{J_L d}{K_D}.$$

The corresponding nondimensionalised boundary and initial conditions are

$$L_2(x = \varepsilon, t) = L_1(x = \varepsilon, t), \quad \frac{\partial L_2(x = \varepsilon, t)}{\partial x} = \frac{\partial L_1(x = \varepsilon, t)}{\partial x}, \quad t > 0, \quad (23)$$

$$\frac{\partial L(x = 0, t)}{\partial t} = Q, \quad L(x = 1, t) = 0, \quad t > 0, \quad (24)$$

$$L_1(x, t = 0) = 0, \quad 0 < x < \varepsilon, \quad L_2(x, t = 0) = 0, \quad \varepsilon < x < 1, \quad (25)$$

$$C(x, t = 0) = 0, \quad 0 < x < \varepsilon. \quad (26)$$

We remark that the parameters α and β are Damköhler numbers, measuring the ratios of timescales for different phenomena, with

$$\alpha = \frac{k_r d^2}{D_L} = \frac{d^2/D_L}{1/k_r},$$

the ratio of the diffusion timescale and the reverse reaction timescale, and

$$\beta = \frac{K d^2}{D_L} = \frac{d^2/D_L}{1/K},$$

the ratio of the diffusion timescale and the ligand decay timescale. We summarise the dimensional parameter values in Table 1 and give the corresponding nondimensional parameter values in Table 2.

Parameter	Meaning	Value
k_f	forward binding rate	$10^3 \text{ m}^3/\text{mole}\cdot\text{s}$
k_r	reverse binding rate	$10^{-6}\text{s}^{-1} < k_r < 10^{-3}\text{s}^{-1}$
K	ligand decay rate	10^{-4}s^{-1}
d	domain length	10^{-3}m
D_L	Diffusion coefficient	$4 \times 10^{-11}\text{m}^2\text{s}^{-1}$
R_0	Initial receptor concentration	$1/3 \times 10^{-3} \text{ moles}/\text{m}^3$
Δx	binding domain length	10^{-6}m
J_F	flux of receptors at $x = 0$	undetermined

Table 1: Values of the dimensional parameters

Parameter	Value
α	$0.025 < \alpha < 25$
β	2.5
γ	$300 < \gamma < 3 \times 10^5$
ϵ	10^{-3}
Q	undetermined

Table 2: Values of the nondimensional parameters

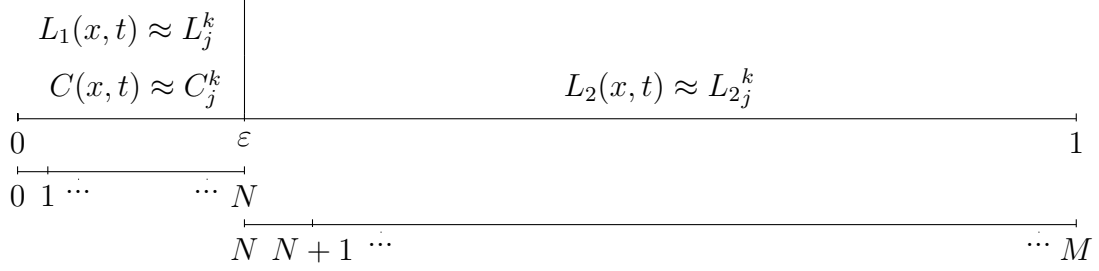


Figure 4: Space discretisation for the finite difference scheme

3.5 Finite difference solution

Having obtained the nondimensional model given by Equations (20)-(26), we are now in a position to seek a numerical solution. We discretise the system of equations on each domain by adopting a forward-time, centred-space difference approximation for L_1 , L_2 , and C . We divide the domain $0 < x < \varepsilon$ into N intervals corresponding to $j = 0, 1, 2, \dots, N$ discrete space points, and divide $\varepsilon < x < 1$ into $M - N$ intervals corresponding to $j = N, N + 1, \dots, M - 1, M$ discrete space points. The lengths of the steps are then given by $\delta x_1 = \frac{\varepsilon}{N}$ for the first interval, and $\delta x_2 = \frac{1-\varepsilon}{M-N}$ for the second interval. We approximate the derivatives of L_1 by

$$\frac{\partial L_1}{\partial t} \approx \frac{L_{1j}^{k+1} - L_{1j}^k}{\delta t}, \quad \frac{\partial^2 L_1}{\partial x^2} \approx \frac{L_{1j-1}^k - 2L_{1j}^k + L_{1j+1}^k}{(\delta x_1)^2},$$

with similar approximations for the derivatives $L_2(x, t)$ and $C(x, t)$, where δt is the timestep to be determined by considering the stability of the method.

Substitution of these approximations into the model equations leads to the system of difference equations

$$L_{1j}^{k+1} = L_{1j}^k + \frac{\delta t}{(\delta x_1)^2} (L_{1j+1}^k - 2L_{1j}^k + L_{1j-1}^k) - \delta t \beta L_{1j}^k - \alpha \delta t [(\gamma - C_j^k)L_{1j}^k - C_j^k], \quad (27)$$

$$C_j^{k+1} = C_j^k + \alpha \delta t [(\gamma - C_j^k)L_{1j}^k - C_j^k], \quad (28)$$

$$L_{2j}^{k+1} = L_{2j}^k + \frac{\delta t}{(\delta x_2)^2} (L_{2j+1}^k - 2L_{2j}^k + L_{2j-1}^k) - \delta t \beta L_{2j}^k. \quad (29)$$

with the boundary and initial conditions

$$\begin{aligned}
L_{11}^{k+1} &= L_{11}^k + \frac{\delta t}{(\delta x_1)^2} (L_{12}^k - 2L_{11}^k - (Q\delta x_1)) - \delta t\beta L_{11}^k - \alpha\delta t [(\gamma - C_1^k)L_{11}^k - C_1^k], \\
L_{1N}^{k+1} &= L_{1N}^k + \frac{\delta t}{(\delta x_1)^2} \left(\left(\frac{L_{22}^k - L_{21}^k}{\delta x_2} \right) \delta x_1 - L_{1N}^k + L_{1N-1}^k \right) \\
&\quad - \delta t\beta L_{1N}^k - \alpha\delta t [(\gamma - C_N^k)L_{1N}^k - C_N^k], \\
L_{1j}^1 &= 0, \\
C_j^1 &= 0, \quad L_{21}^{k+1} = L_{1N}^{k+1}, \\
L_{2M-N+1}^k &= 0, \quad L_{2j}^1 = 0.
\end{aligned}$$

The equation determining the timestep is

$$\delta t = CFL \cdot \frac{1}{\frac{2}{\min\{\delta x_1, \delta x_2\}^2} - \alpha\gamma - \beta},$$

where $CFL = 0.9$ is chosen to satisfy the *Courant-Friedrichs-Lewy condition* for convergence, which in this case reads $CFL \leq 1$.

3.6 The method of lines

The method of lines is a semi-analytical method for numerically solving PDEs, whereby PDEs are converted into ODEs by discretising in only one direction (here, space) using finite different methods while using analytical solutions in the remaining direction (time). This leads to efficient computations, easier stability and convergence conditions, reduced programming effort and reduced computational time.

Applying the method of lines to Equations (20-21) we get the system of ODEs

$$\frac{dL_1}{dt} = \frac{1}{(\delta x_1)^2} (L_{1j+1} - 2L_{1j} + L_{1j-1}) - \beta L_{1j} - \alpha [(\gamma - C_j)L_{1j} - C_j], \quad (30)$$

$$\frac{dC}{dt} = \alpha [(\gamma - C_j)L_{1j} - C_j], \quad (31)$$

$$\frac{dL_2}{dt} = \frac{1}{(\delta x_2)^2} (L_{2j+1} - 2L_{2j} + L_{2j-1}) - \beta L_{2j}. \quad (32)$$

The associated boundary conditions are given by the ODE

$$\frac{dL_1}{dt} = \frac{1}{(\delta x_1)^2} (2L_{12} - 2L_{11} - 2(Q\delta x_1)) - \beta L_{11} - \alpha [(\gamma - C_1)L_{11} - C_1] \text{ at } x = 0, \quad (33)$$

and the three algebraic equations

$$L_{1N} = L_{1N-1} + \frac{\delta x_1}{\delta x_2} (L_{22} - L_{21}) \text{ at } x = \varepsilon, \quad (34)$$

$$L_{1N} = L_{21} \text{ at } x = \varepsilon, \quad (35)$$

$$L_{2N} = 0 \text{ at } x = 1, \quad (36)$$

and the initial conditions are

$$L_{1j} = C_j = L_{2j} = 0. \quad (37)$$

3.7 Some limiting cases

Here we seek to simplify the model equations by examining the values of the parameters appearing in the model. Observing that the product $\alpha\gamma$, measuring the ratio of the diffusion timescale and the forward reaction timescale, has value $7500 \gg 1$, it is clear that binding occurs on a much faster timescale than diffusion. We use this *rapid binding* approximation to reduce the coupled system of equations in $0 < x < \varepsilon$ to a single PDE with effective concentration-dependent diffusivity. Dividing Equation (21) by $\alpha\gamma$ and setting the left-hand side equal to zero gives

$$\left(1 - \frac{C}{\gamma}\right) L - \frac{C}{\gamma} = 0, \quad (38)$$

which we rearrange to obtain

$$C(L) = \frac{\gamma L}{1 + L}. \quad (39)$$

Adding Equations (20) & (21) produces

$$\frac{\partial T}{\partial t} = \frac{\partial^2 L}{\partial x^2} - \beta L. \quad (40)$$

where we define T to be the total concentration of complexes and unbound ligands,

$$T = L + C(L). \quad (41)$$

Using the chain rule, we rewrite Equation (40) as

$$\frac{\partial T}{\partial t} = \frac{\partial}{\partial x} \left(\frac{dL}{dT} \frac{\partial T}{\partial x} \right) - \beta L \quad (42)$$

It remains to calculate $\frac{dL}{dT}$. Substituting the expression for $C(L)$ obtained in Equation (39) into Equation (41) and rearranging gives a quadratic equation for L , which has solutions

$$L = -\frac{1}{2}(1 + \gamma - T) \pm \frac{1}{2}\sqrt{(1 + \gamma - T)^2 + 4T}. \quad (43)$$

We take the positive case, since the negative case does not give a physically meaningful solution. Differentiating this with respect to T gives

$$\frac{dL}{dT} = \frac{1}{2} + \frac{(T - \gamma + 1)}{2\sqrt{(1 + \gamma - T)^2 + 4T}} = W(T), \quad (44)$$

which gives

$$\frac{\partial T}{\partial t} = \frac{\partial}{\partial x} \left(W(T) \frac{\partial T}{\partial x} \right) - v(T), \quad (45)$$

where $W(T) = \frac{dL(T)}{dT}$ is the concentration-dependent diffusivity. Thus in the limit $\alpha\gamma \gg 1$, the system of coupled equations (20)-(21) reduces to the single equation (45) for the concentration-dependent diffusivity. The evolution of the concentration-dependent diffusivity $W(T)$ for various values of γ is shown in Figure 5. Finally, we consider the two limiting cases when $\gamma = 0$ and $\gamma \rightarrow \infty$. When $\gamma = 0$, we have

$$\frac{\partial L}{\partial T} = 1,$$

and the equation governing $W(T)$ then reduces to

$$\frac{\partial T}{\partial t} = \frac{\partial^2 T}{\partial x^2} - \beta L,$$

so that diffusion and ligand decay dominate. On the other hand, when $\gamma \rightarrow \infty$, we have

$$\frac{\partial L}{\partial T} = 0$$

and the equation governing $W(T)$ reduces to

$$\frac{\partial T}{\partial t} = -\beta L,$$

so that ligand decay is the dominant phenomenon.

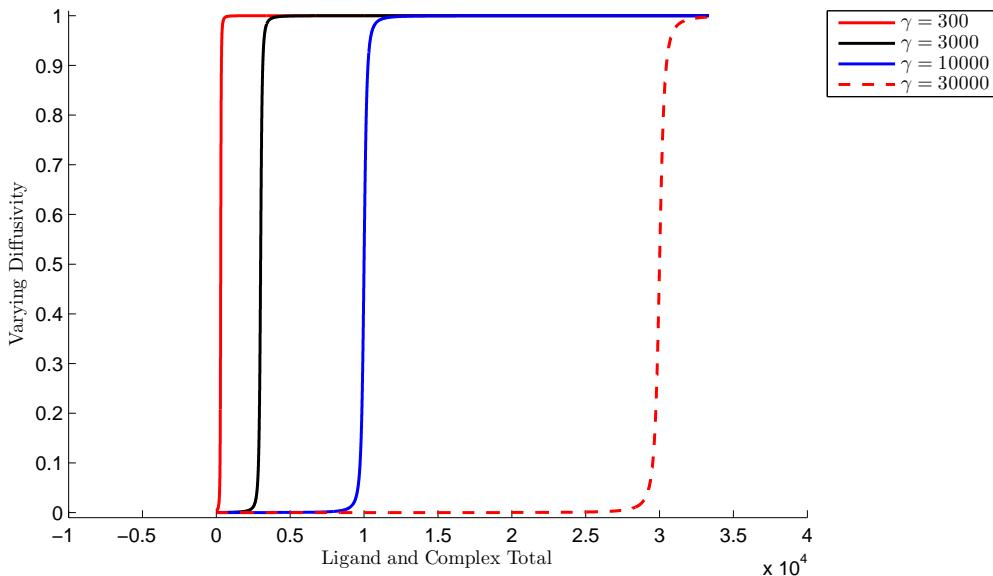


Figure 5: Evolution of diffusivity $W(T)$ for various values of γ

4 Results

4.1 Receptor occupancy

Using Equation (5), we may calculate the time taken to reach a receptor occupancy of 90% initial concentration, that is, $C^* = 0.9R_T$. Taking, for example, $L_0/K_D = 300$ gives a time of approximately 8 s for $k_r = 10^{-3} \text{ s}^{-1}$ and a time of approximately 2 hours for $k_r = 10^{-6} \text{ s}^{-1}$. A log-log plot of time taken to reach 90% receptor occupancy for various values of L_0/K_D is given in Figure 6.

4.2 Model results

The nondimensional model obtained in Section 3.4 was solved numerically using the finite difference method outlined in Section 3.5. The results obtained are shown in Figures 7 and 8, where we have plotted $L_1(x, t)/\gamma$, $L_2(x, t)/\gamma$, and $C(x, t)/\gamma$. The model equations were also solved using the method of lines, described in Section 3.6. The system of differential algebraic equations (30-37) was solved using the built-in Matlab function `ode15s`, a variable-step, variable-order (VSVO) solver based on numerical differentiation formulas of orders 1 to 5. The solutions obtained for $L_1(x, t)$, $L_2(x, t)$, and $C(x, t)$, with $N = M = 101$, are shown in Figures 9a-9c.

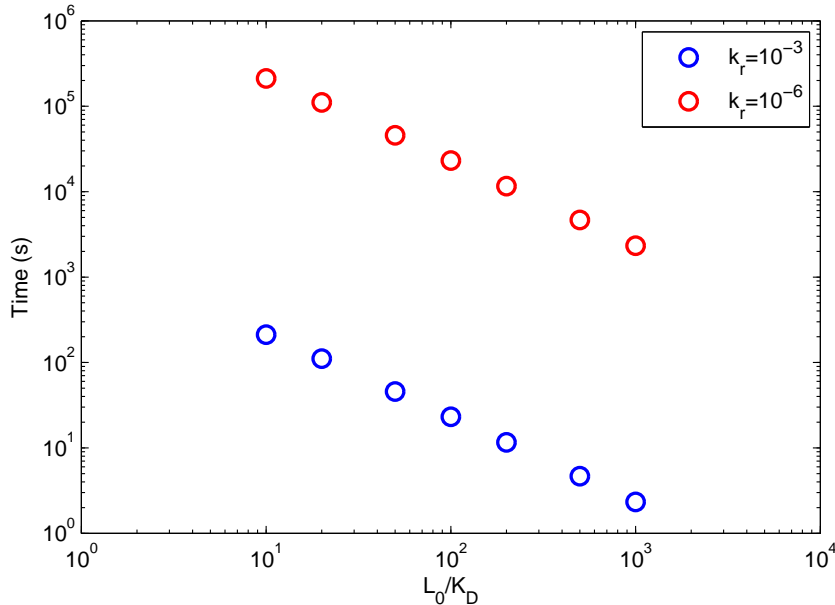


Figure 6: Log-log plot of time taken to reach 90% receptor occupancy for various values of L_0/K_D , and for $k_r = 10^{-3} s$, $k_r = 10^{-6} s$

5 Conclusions and Future Work

In this report, we have developed a model accounting for receptor-ligand binding and ligand diffusion and decay. We have used a finite difference method to solve the full non-linear model equations, and we have also examined some limiting cases of the model. The results obtained in each stage agree with expected behaviour as observed experimentally. Future work and further iterations of the model should include the role of antibodies. Further insights might be gained by taking the diffusivity and flux to be variable instead of fixed quantities. The model could also be expanded to account for paracrine and endocrine signalling, which has not been examined here.

Acknowledgements. We wish to sincerely acknowledge Dr Armin Sepp of GSK for his valuable advice and support throughout the workshop. We are very grateful to our academic mentor, Dr Sean McGinty, for his guidance and encouragement, and we also thank him for leading the organisation of the workshop. Funding received from MI-NET, the Mathematics for Industry Network COST Action, is gratefully acknowledged.

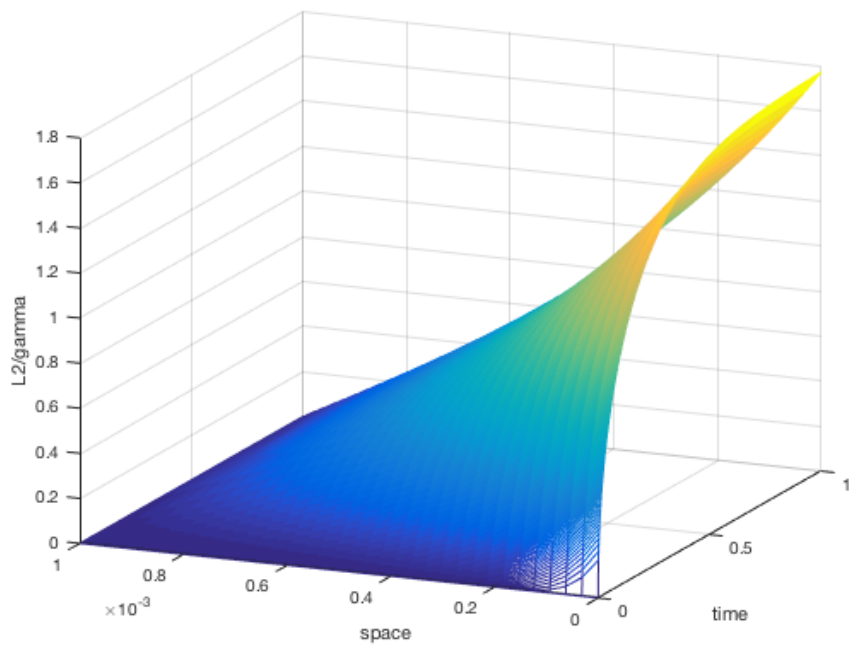
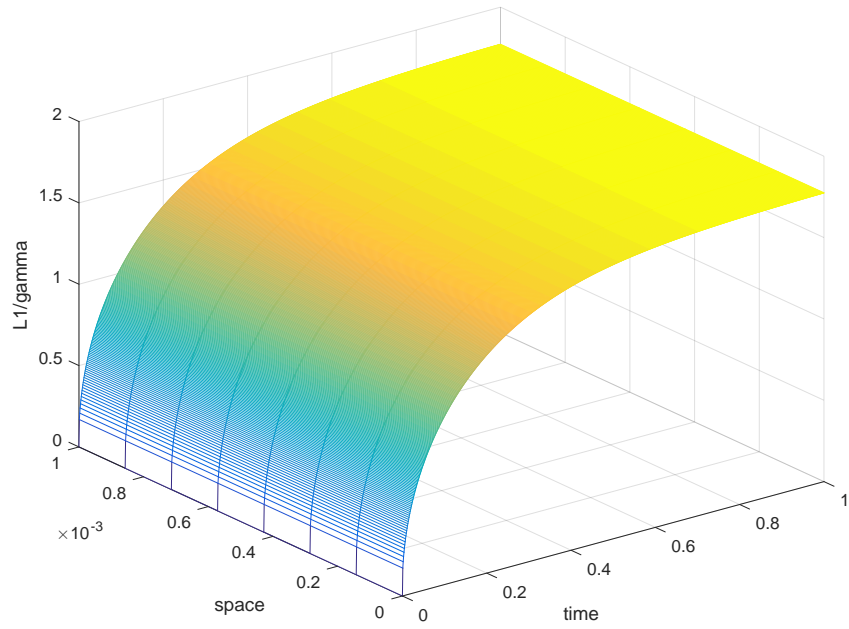


Figure 7: Finite difference solution for evolution of $L_1(x,t)/\gamma$ (left) and $L_2(x,t)/\gamma$ (right), with $\alpha = 25$, $\gamma = 300$, $N = 8$, $M = 40$

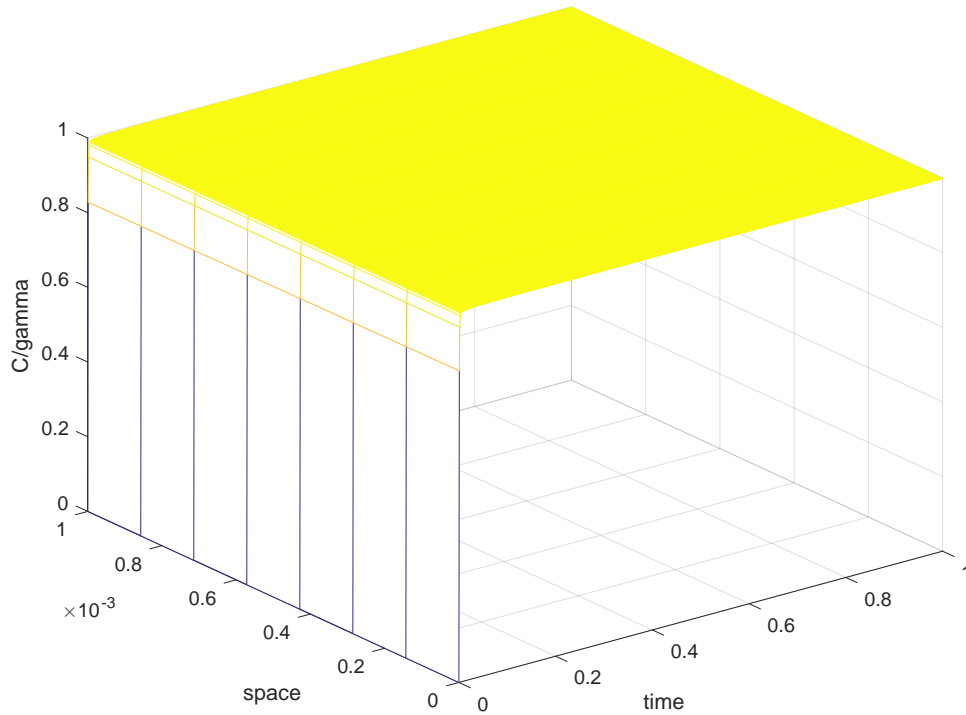
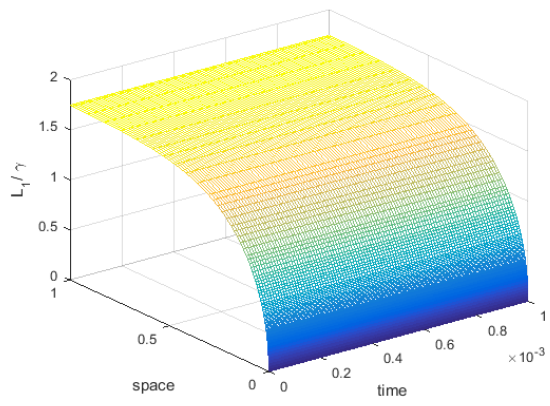


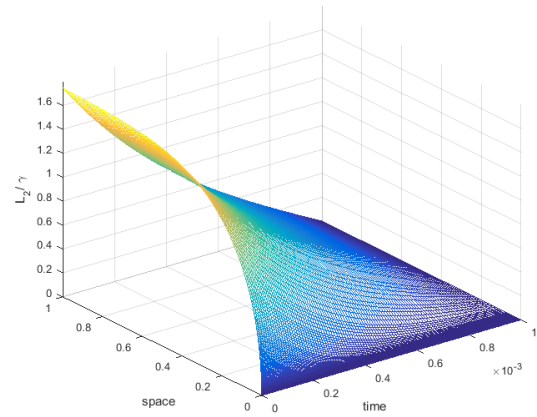
Figure 8: Finite difference solution for evolution of $C(x, t)/\gamma$ with $\alpha = 25$, $\gamma = 300$, $N = 8$, $M = 40$

References

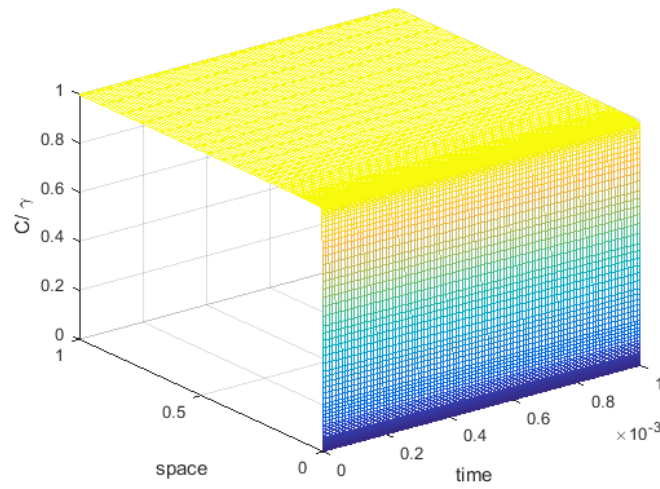
- [1] P. Chames, et al., Therapeutic antibodies: successes, limitations and hopes for the future, *Br. J. Pharmacol.*, 2(157):220–233 (2009).
- [2] A. C. Chan, et al., Therapeutic antibodies for autoimmunity and inflammation, *Nat. Rev. Immunol.*, 10:301–316 (2010).
- [3] E. B. Rodrigues, et al., Therapeutic monoclonal antibodies in ophthalmology, *Progress in Retinal and Eye Research*, 28:117–144 (2009).
- [4] H. W. Schroeder, et al., Structure and function of immunoglobins, *J. Allergy Clin. Immunol.*, 125(202):41–52 (2010).
- [5] D. L. Muller, et al., Clonal expansion versus functional clonal inactivation: a costimulatory signalling pathway determines the outcome of T cell antigen receptor occupancy, *Ann. Rev. Immunol.*, 7:445–480 (1989).



(a) Evolution of $L_1(x, t)$



(b) Evolution of $L_2(x, t)$



(c) Evolution of $C(x, t)$

Figure 9: Results from the method of lines, with $N = M = 101$